DEVELOPMENT AND DISEASE

The regional pattern of retinoic acid synthesis by RALDH2 is essential for the development of posterior pharyngeal arches and the enteric nervous system

Karen Niederreither[2], Julien Vermot[1], Isabelle Le Roux[1], Brigitte Schuhbaur[1], Pierre Chambon[1] and Pascal Dollé[1,*]

[1]Institut de Génétique et de Biologie Moléculaire et Cellulaire, CNRS/INSERM/ULP/Collège de France, BP 10142, 67404 Illkirch Cedex, CU de Strasbourg, France
[2]Departments of Medicine and Molecular and Cellular Biology, Center for Cardiovascular Development, Baylor College of Medicine, One Baylor Plaza, Houston, Texas 77030, USA
*Author for correspondence (e-mail: dolle@igbmc.u-strasbg.fr)

SUMMARY

Targeted inactivation of the mouse retinaldehyde dehydrogenase 2 (RALDH2/ALDH1a2), the enzyme responsible for early embryonic retinoic acid synthesis, is embryonic lethal because of defects in early heart morphogenesis. Transient maternal RA supplementation from E7.5 to (at least) E8.5 rescues most of these defects, but the supplemented *Raldh2*^{−/−} mutants die prenatally, from a lack of septation of the heart outflow tract (Niederreither, K., Vermot, J., Messaddeq, N., Schuhbaur, B., Chambon, P. and Dollé, P. (2001). *Development* 128, 1019-1031). We have investigated the developmental basis for this defect, and found that the RA-supplemented *Raldh2*^{−/−} embryos exhibit impaired development of their posterior (3rd-6th) branchial arch region. While the development of the first and second arches and their derivatives, as well as the formation of the first branchial pouch, appear to proceed normally, more posterior pharyngeal pouches fail to form and the pharyngeal endoderm develops a rudimentary, pouch-like structure. All derivatives of the posterior branchial arches are affected. These include the aortic arches, pouch-derived organs (thymus, parathyroid gland) and post-otic neural crest cells, which fail to establish segmental migratory pathways and are misrouted caudally. Patterning and axonal outgrowth of the posterior (9th-12th) cranial nerves is also altered. Vagal crest deficiency in *Raldh2*^{−/−} mutants leads to agenesis of the enteric ganglia, a condition reminiscent of human Hirschprung's disease. In addition, we provide evidence that: (i) wildtype *Raldh2* expression is restricted to the posteriormost pharyngeal mesoderm; (ii) endogenous RA response occurs in both the pharyngeal endoderm and mesoderm, and extends more rostrally than *Raldh2* expression up to the 2nd arch; (iii) RA target genes (*Hoxa1*, *Hoxb1*) are downregulated in both the pharyngeal endoderm and mesoderm of mutant embryos. Thus, RALDH2 plays a crucial role in producing RA required for pharyngeal development, and RA is one of the diffusible mesodermal signals that pattern the pharyngeal endoderm.

Key words: Retinoids, Branchial arches, Pharyngeal endoderm, DiGeorge syndrome, Hirschprung's disease, Mouse mutant

INTRODUCTION

Conotruncal and aortic arch malformations are prevalent human birth defects. Septation of the outflow tract into aorta and pulmonary artery which, when defective, leads to persistent truncus arteriosus (PTA), involves a specific population of neural crest cells (NCCs), called 'cardiac NCCs'. These cells migrate from the hindbrain rhombomeres (r) r6, r7 and r8 to populate the posterior (3rd, 4th and 6th) branchial arches, eventually contributing to the aorticopulmonary septum and conotruncal ridges (Kirby, 1998; Jiang et al., 2000). Surgical ablation of premigratory cardiac NCCs in chick embryos produces a range of abnormal phenotypes including PTA, overriding aorta, and ventricular septal defects (Creazzo

et al., 1998). Severe vitamin A deficiency in rodents can also lead to alterations of NCC derivatives, resulting in similar congenital malformations (Wilson and Warkany, 1949). The active derivatives of vitamin A, the retinoic acids (RAs), act as agonistic ligands for RA receptors (all-*trans* and 9-*cis* RAs for RARα, β and γ) and retinoid X receptors (9-*cis* RAs for RXRα, β and γ), which bind as heterodimers to DNA motifs (RA response elements, RAREs) and thus regulate the transcriptional activity of target genes (reviewed by Mangelsdorf et al., 1994; Chambon, 1996). Compound inactivation of RARα and RARβ leads to various abnormalities, including abnormal patterns of branchial arch-derived great arteries and defective septation of the outflow tract (Mendelsohn et al., 1994; Ghyselinck et al., 1998). These

double mutant mice exhibit abnormal patterning of the post-otic hindbrain and the caudal (3rd-6th) branchial arches (Dupé et al., 1999). In this respect, it is noteworthy that administration of a pan-RAR antagonist to cultured mouse embryos revealed a selective sensitivity of the caudal branchial region to inhibition of RA signaling during the period of NCC migration (Wendling et al., 2000).

Interestingly, *Raldh2*$^{-/-}$ null mutant embryos, which are severely impaired in their capacity to synthesize RA, die at midgestation (E9.5-10.5) because of severe defects of early heart morphogenesis (Niederreither et al., 1999; Niederreither et al., 2001). These mutant embryos also exhibit an altered development of trunk mesoderm derivatives, as well as growth and patterning defects of the posterior hindbrain region and an apparent lack of development of all branchial arches, with the exception of the first one (Niederreither et al., 1999; Niederreither et al., 2000). Several of these abnormalities have been shown to be rescued through maternal RA supplementation from embryonic day 7.5 (E7.5) to at least E8.5 (Niederreither et al., 1999; Niederreither et al., 2002). These rescued *Raldh2*$^{-/-}$ mutants consistently exhibit outflow tract septation defects (PTA), which most probably account for their death prior to (or at) birth, and extending the duration of RA supplementation (e.g. until E10.5 or 12.5) has no effect on the septation defect (Niederreither et al., 2001).

We have determined here the defective developmental events that lead to PTA in the RA-supplemented *Raldh2*$^{-/-}$ mutants, and have characterized a number of additional abnormalities exhibited by these rescued mutants. Most notably, we show for the first time that RA deficiency can lead to a Hirschprung disease-like phenotype (agenesis of the enteric ganglia) due to vagal crest deficiency.

MATERIALS AND METHODS

The generation of *Raldh2*-null mutant mice has been described previously (Niederreither et al., 1999). The defects investigated in this study were obtained after RA supplementation of the maternal food: all-*trans*-RA (Sigma) from a 5 mg/ml ethanol stock suspension was diluted in 50 ml water and mixed with 30 g powdered food (R03 breeding diet from UAR, Villemoisson, France) at a final concentration of 100 µg/g food (E7.5 to 8.5) or 250 µg/g (E8.5 onwards). The resulting food paste was provided daily to the pregnant mice in a Petri dish wrapped in aluminium foil. Most analyses (except histology, see below) were performed on embryos that were RA-supplemented from E7.5 to E9.5. Some experiments were also performed on embryos that were supplemented until the day of sacrifice. Extending the RA supplementation did not significantly improve the *Raldh2*$^{-/-}$ phenotype (see Results).

Whole-mount in situ hybridizations were performed as described previously (Décimo et al., 1995), using template plasmids cloned in our Institute or kindly provided by Drs G. Barsh (Stanford University, CA; *kreisler/Mafb*), P. Gruss (MPI, Göttingen; *Pax1*, *Pax9*), R. Krumlauf (Stowers Institute, Kansas City, MI; *Hoxa2*) G. Martin (UC San Fransisco, CA; *Fgf8*). Whole-mount X-gal assays of embryos carrying a *RARE-hsp68-lacZ* reporter transgene, which harbors a tetrameric repeat of the *RARβ2* RARE linked to the *hsp68* minimal promoter, were performed as described previously (Rossant et al., 1991). Anti-neurofilament staining with the 2H3 monoclonal antibody (Developmental Studies Hybridoma Bank, Iowa City, IA) and in situ hybridization on cryosections were performed as described previously (Mark et al., 1993; Niederreither and Dollé, 1998).

RESULTS

RA-rescued *Raldh2*$^{-/-}$ embryos exhibit defects of posterior branchial arch derivatives

Histological analysis was performed on E18.5 *Raldh2*$^{-/-}$ mutants after RA rescue from E7.5-E12.5, to see whether their heart septation defect (PTA; see Fig. 1B) correlated with defects of other branchial arch derivatives. The embryonic pharyngeal pouches give rise to several derivatives, including the thymus and parathyroid glands, which derive from the 3rd and 4th pouches, respectively (Larsen, 1997). Some of the RA-rescued *Raldh2*$^{-/-}$ mutants lacked the thymus gland (compare Fig. 1A and B). Others had ectopic thymic rudiments in their cervical region, adjacent to the thyroid tissue (Fig. 1C,F). Furthermore, no parathyroid glands were seen along the lateral wall of the thyroid lobes (compare Fig. 1D-F). Thus, defects of pharyngeal pouch-derived organs are associated with heart outflow tract septation defects in the RA-rescued *Raldh2*$^{-/-}$ mice. This condition is reminiscent of the defects seen in human DiGeorge syndrome (Scambler, 2000; Emanuel, 2001; Lindsay, 2001) and in recently generated mouse models for this syndrome (Lindsay et al., 2001; Merscher et al., 2001) (see Discussion).

When collected at E9.5, RA-rescued *Raldh2*$^{-/-}$ embryos exhibited a lack of discernible 3rd branchial arches, whereas their 1st and 2nd arches were of normal size (e.g. Fig. 3G-L). Embryonic intracardiac ink injections were performed at various developmental stages, to analyze aortic arch development in the rescued *Raldh2*$^{-/-}$ mutants. At E9.5, the mutant embryos appeared to lack the 3rd aortic arches, whereas the 2nd aortic arches were well formed (Fig. 2A,B). At E10.5 in wild-type embryos, ink injection mostly labels the 3rd and 4th aortic arches, as the 2nd arches are being remodelled (Fig. 2C). E10.5 *Raldh2*$^{-/-}$ embryos had no visible 3rd or 4th aortic arches, and the labeled arterial flow mostly passed through their 2nd arches (Fig. 2D). At E11.5, the 3rd, 4th and 6th aortic arches are labeled in wild-type embryos (Fig. 2E). In contrast, a single arterial vessel connected the aortic sac and the dorsal aortae in *Raldh2*$^{-/-}$ embryos (Fig. 2F). This abnormal arch was very poorly developed in some specimens (inset in Fig. 2F). The aortic arch defects were observed in mutants after short-term (E7.5-E9.5) or long-term (until day of analysis) RA supplementation.

RA supplementation does not properly restore RA levels in the prospective branchial arch region of *Raldh2*$^{-/-}$ embryos

Raldh2 is known to be expressed in various mesodermal derivatives, from gastrulation onwards (Niederreither et al., 1997). We analyzed how its expression is related to branchial arch development in wild-type embryos. At E8.5 (10-12 somite pairs), when only the first branchial arch and first pharyngeal pouch are visible, *Raldh2* was expressed in the splanchnic mesoderm up to a boundary located towards the posterior extremity of the foregut pocket (Fig. 2E, arrowhead). While *Raldh2* expression levels decreased in the various trunk mesodermal derivatives (e.g. in somites) by ~E8.75, a specific expression domain persisted caudally to the foregut pocket (Fig. 2F). This domain remained distant from the developing 3rd pharyngeal pouch, i.e. was restricted to the posteriormost area of the prospective branchial arch region. Bisection of the
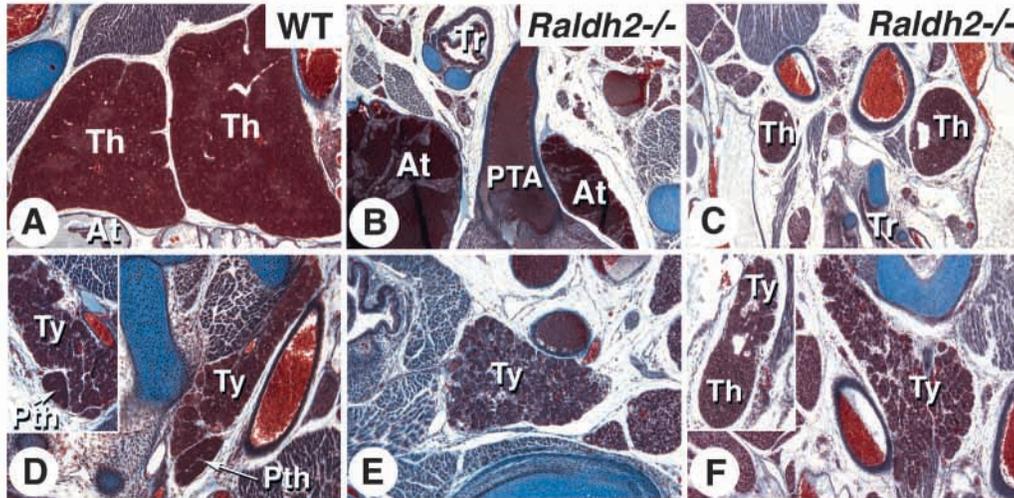
Fig. 1. Thymus and parathyroid defects in RA-rescued *Raldh2*−/− mutants. Coronal histological sections (stained with tetrachrome) of an E18.5 wild-type fetus (WT; A,D) and two *Raldh2*−/− fetuses (B,E and C,F) that were rescued by maternal RA supplementation from E7.5 to E12.5. (A) A representative section of the wild-type thymus gland. (D) Sections of the left and right thyroid lobes and the adjacent parathyroid glands. (B) No thymus was seen in the mediastinum of the first mutant (note the presence of a persistent truncus arteriosus). (C) An ectopic cervical thymus rudiment was found in the second animal. (E-F) This rudiment was connected to the thyroid tissue via a pouch-like structure (F, inset). No parathyroid glands were seen in the mutants. At, atrium; PTA, persistent truncus arteriosus; Pth, parathyroid; Th, thymus; Tr, trachea; Ty, thyroid.
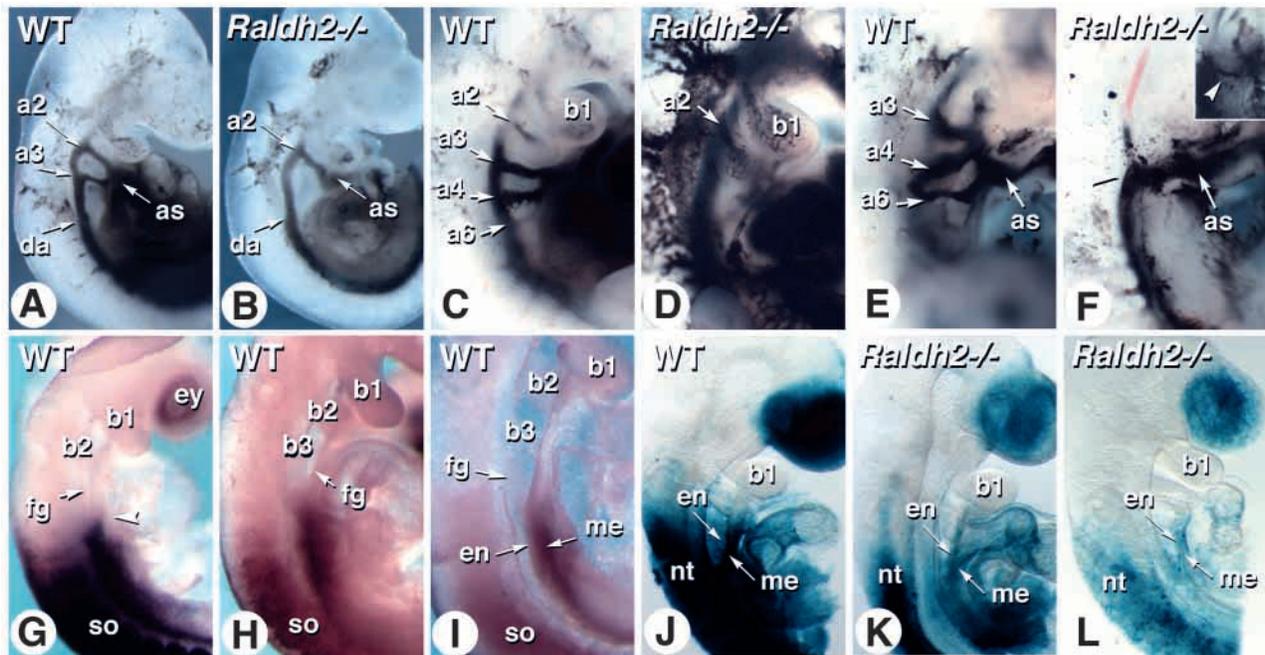

Fig. 2. (A-F) Defects in aortic arch formation in RA-rescued *Raldh2*−/− embryos. Embryos collected at E9.5 (A,B), E10.5 (C,D) or E11.5 (E,F) were incubated in phosphate-buffered saline and injected intracardially with china ink. Compare the aortic arch patterns in wild-type (A,C,E) and *Raldh2*−/− (B,D,F) embryos (see text for details). The inset in F shows a detail of a different *Raldh2*−/− embryo. Arrowheads point to the single embryonic vessel connecting the aortic sac and the dorsal aorta. (G-I) Analysis of *Raldh2* expression pattern in the wild-type embryonic pharyngeal region. Whole-mount in situ hybridization of an antisense *Raldh2* riboprobe was performed on E8.5 (~10 somites, G) and E8.75 (~16 somites, H,I) wild-type embryos. The arrowhead in G points to *Raldh2* expression boundary in the posterior foregut region. (I) A higher magnification of the branchial arch region, viewed from the inside after bisection of the embryo. (J-L) Patterns of RA response in the branchial arch region of E8.5 wild-type (J) and *Raldh2*−/− (K,L) embryos carrying a RARE-hsp68-*lacZ* reporter transgene. Embryos are shown after whole-mount X-gal assay and medial bisection of their head and trunk region (inside views). a2-a6, aortic arches; as, aortic sac; b1-b3, branchial arches; da, dorsal aorta; en, endoderm; ey, eye; fg, foregut; me, mesoderm; nt, neural tube; so, somites.

embryos revealed expression in the mesoderm underlying the ventral aspect of the foregut endoderm, rather than in the endoderm itself (Fig. 2G).

Interestingly, this expression pattern did not really match the spatial activity of a RA-inducible reporter transgene (Rossant et al., 1991) (see Materials and Methods). In wild-type E8.5 embryos, the reporter transgene was expressed at high levels along the foregut wall, up to the posterior edge of the developing 2nd arch (Fig. 2H). Furthermore, the RA-reporter transgene was activated in both the endodermal and mesodermal layers of the foregut pocket (Fig. 2H). RA-reporter activity also extended further rostrally in the dorsal (hindbrain-adjacent) mesenchyme up to the otocyst level (Fig. 2H), whereas *Raldh2* transcripts did not reach the otocyst (Fig. 2E,F).

RA-reporter transgene activity was clearly weaker in the RA-rescued *Raldh2*$^{-/-}$ mutant embryos (Fig. 2I,J) although its spatial distribution was comparable to that seen in wild-type embryos (Fig. 2H). Downregulation was seen in both the endodermal and mesodermal layers of the foregut. In the most severe cases, expression was restricted to scattered cells in the branchial region and the hindbrain mesenchyme (Fig. 2J). However, these cells extended almost as rostrally as in wild-type embryos (Fig. 2H).

Impairment of endodermal and mesodermal foregut gene expression in rescued *Raldh2*-null mutants

The homeobox genes *Hoxa1* and *Hoxb1* are known to be RA-regulated, both in vitro and in vivo, through RAREs located in their regulatory regions (Gavalas et al., 1998). Expression of both genes was selectively downregulated in the foregut region of the RA-rescued *Raldh2*$^{-/-}$ embryos (Fig. 3A-F). Downregulation was seen in both the endoderm and mesoderm of the posterior foregut (compare Fig. 3C,E and D,F). Expression of both genes in the tail bud and posterior trunk tissues, as well as *Hoxb1* expression in the 4th rhombomere (r4), was not detectably altered in the mutant embryos (Fig. 3A,B, and data not shown).

FGF8 is a signaling molecule expressed in specific regions of the wild-type branchial arch ectoderm and endoderm (Crossley and Martin, 1995; Wall and Hogan, 1995). Within the endoderm, *Fgf8* expression is highest at the level of the developing pharyngeal pouches (Fig. 3I). *Fgf8* was expressed at abnormally low levels along the posterior branchial arch region of E9.5 *Raldh2*$^{-/-}$ embryos, and its spatial distribution was altered. Scattered ectodermal *Fgf8*-expressing cells were observed in mutant embryos from the level of the 2nd-3rd branchial cleft down to ectopic posterior locations, almost reaching the level of the forelimb bud rudiment (compare Fig. 3G and H, bracket). Furthermore, there was almost no detectable *Fgf8* expression in the mutant pharyngeal endoderm, except at the level of the developing 2nd pouch (compare Fig. 3I and J). The distribution and levels of expression of *Fgf8* were unaltered in the first branchial arch, as well as in other craniofacial regions, of the mutant embryos (Fig. 3H,J, and data not shown).
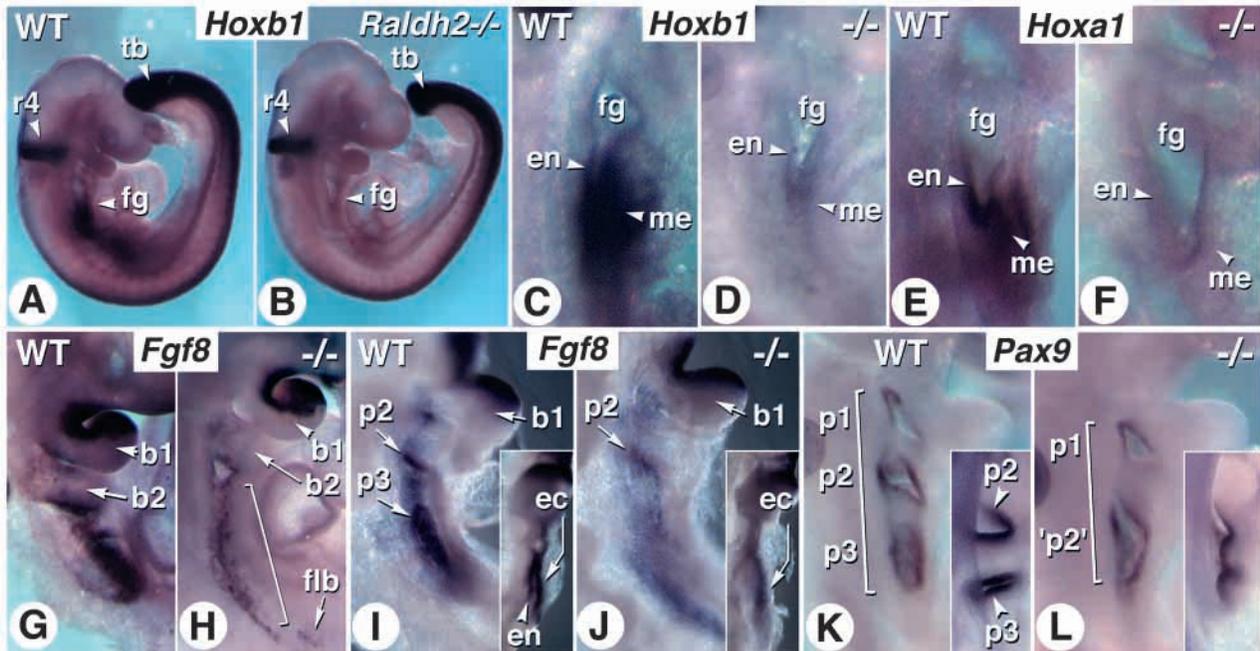

Fig. 3. Altered gene expression in the posterior pharyngeal region of RA-rescued *Raldh2*$^{-/-}$ embryos. (A-D) Whole-mount in situ analysis of *Hoxb1* transcripts in E9 (~22 somites) wild-type (A,C) and *Raldh2*$^{-/-}$ (B,D) embryos. Profile views of the whole embryos (A,B) and enlargement of the posterior foregut region after medial bisection (C,D, inside views). (E,F) In situ hybridization analysis of *Hoxa1* transcripts in the foregut area of E9 wild-type and *Raldh2*$^{-/-}$ embryos, respectively (viewed as in C,D). (G-J) In situ hybridization analysis of *Fgf8* transcripts in E9.5 wild-type (G,I,) and *Raldh2*$^{-/-}$ (H,J) embryos. External profile views (G,H) show *Fgf8* ectodermal labeling, whereas internal views after bisection (I,J) reveal the endodermal labeling. Insets in (I,J) are coronal views which make it possible to distinguish the ectodermal and endormal labeling. (K,L) In situ hybridization analysis of *Pax9* expression in the foregut region of E9.5 (main panels) and E10.5 (insets: detail of the pharyngeal region caudally to the 2nd arch) wild-type and *Raldh2*$^{-/-}$ embryos, respectively. b1-b3, branchial arches; ec, ectoderm; en, endoderm; fg, foregut; me, mesoderm; p1-p3, pharyngeal pouches; r4, rhombomere 4; tb, tail bud.

We also analyzed *Pax1* and *Pax9* transcript distributions in mutant embryos, as these genes are differentially expressed along the endoderm of the developing pharyngeal pouches (Müller et al., 1996). Both *Pax1* (data not shown) and *Pax9* (Fig. 3K,L) expression patterns confirmed the lack of a distinct 3rd pharyngeal pouch and the formation of a single, enlarged 2nd pouch in E9.5 mutant embryos (Fig. 3L, 'p2'). Despite this abnormality, *Pax9* was differentially expressed along the dorsoventral axis of the mutant 2nd pouch, in a pattern similar to that seen in the wild-type 2nd and 3rd pouches (compare Fig. 3K and L). Note that the overall size of the pharyngeal pouch region (from the anterior aspect of the 1st pouch to the posterior aspect of the abnormal 2nd pouch) was clearly reduced in E9.5 mutant embryos (Fig. 3K,L, brackets). Mutants collected at E10.5 after RA supplementation (from E7.5 to E9.5 or E10.5) similarly showed fused pouch-like rudiments caudally to their 2nd branchial arches (compare Fig. 3K and L, insets).

Neural crest cell migration is abnormal in rescued *Raldh2*-null mutants

Several neural crest markers were used to investigate whether the abnormal development of posterior branchial arches in rescued *Raldh2*⁻/⁻ embryos correlated with NCC defects. The *EphA4* gene is normally expressed in r3 and r5, and in NCC emanating from the latter rhombomere (Nieto et al., 1992) (Fig. 4A). *EphA4* was expressed at normal levels in r3 and r5 of *Raldh2*⁻/⁻ embryos (compare Fig. 4A and B). However, the stream of NCC that colonized the 3rd arch in wild-type embryos had no counterpart in mutants (Fig. 4B). The *EphA2* gene is expressed in wild-type embryos in both NCC and mesodermal cells of the post-otic region and 3rd-6th pharyngeal arches (Ruiz and Robertson, 1994) (Fig. 4C). *EphA2*-expressing cells were detected in *Raldh2*⁻/⁻ embryos, but these cells remained confined dorsally to the foregut pocket (Fig. 4D, arrowhead).

Cellular RA binding protein 1 (*Crabp1*) gene transcripts

mark migratory and early post-migratory NCC at all craniofacial levels (Maden et al., 1992). *Crabp1*-labeled cells colonized the 2nd arch, as well as more rostral facial regions of *Raldh2*⁻/⁻ embryos (Fig. 2F,G), to the same extent as in wild-type embryos (Fig. 4E). *Crabp1*-positive cells were also found caudally to the 2nd arch in mutant embryos, but these cells failed to migrate along organized segmental pathways and extended more caudally than in wild-type embryos, eventually merging with the trunk and forelimb labeled cells (Fig. 4F,G, brackets). *Crabp1* labeling also revealed abnormal patterns of connectivity between the post-otic hindbrain and the corresponding post-migratory NCC. In wild-type embryos, two main streams connect the hindbrain and the 3rd-4th arch NCC populations (Fig. 4H, arrowheads). *Raldh2*⁻/⁻ embryos exhibited several 'segmental-like' streams extending from r6 down to the spinal cord levels (Fig. 4I).

Abnormal development of posterior cranial nerves in rescued *Raldh2*-null mutants

The patterning of cranial nerves, which develop within specific branchial arches, was analyzed at E11.5 in *Raldh2*⁻/⁻ mutants that were RA-rescued from E7.5-E9.5, using anti-neurofilament immunostaining (Fig. 5). Patterning of the nerves that develop in the 1st and 2nd branchial arches (5th and 7th cranial nerves, respectively) was normal in most of the mutant embryos (Fig. 5B-D). All mutants, however, showed impaired development of the 9th (glossopharyngeal) and 10th (vagus) nerves, which normally develop within the 3rd and 4th branchial arches. Three examples of phenotypes of increasing severity are shown in Fig. 5B-D. In the less severe cases, separate 9th and 10th nerve tracts were formed, but their connections with the hindbrain were mingled (Fig. 5B). In addition, the distal sensory ganglia of these nerves, which normally derive from the 2nd and 3rd epibranchial placodes, were abnormally fused (Fig. 5B). In more severe cases, the axon bundles of presumptive 9th and 10th nerves merged in a single rudimentary trunk that followed an aberrant route (Fig.
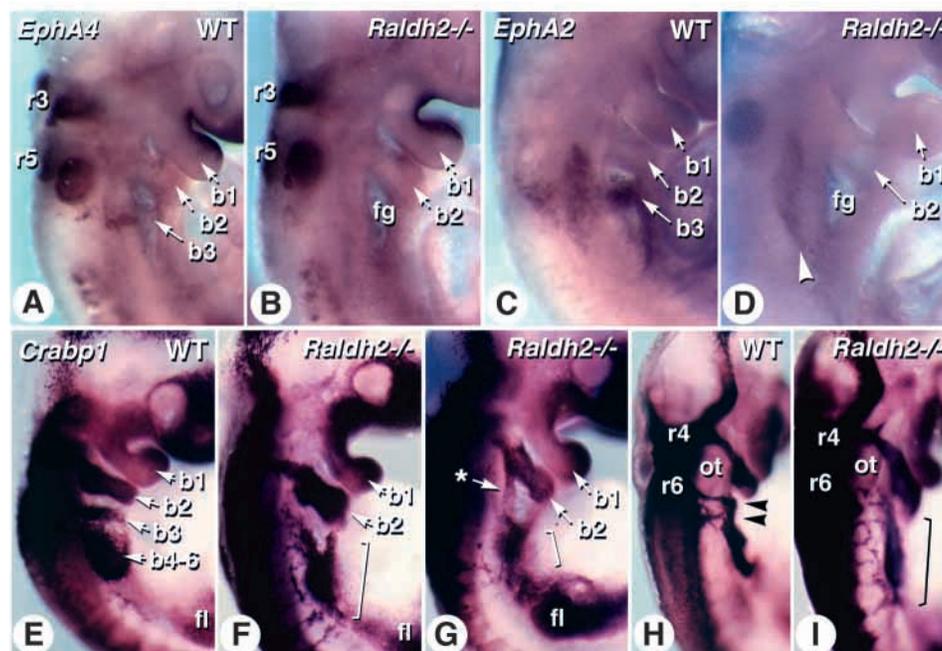

Fig. 4. Post-otic neural crest cell alterations in RA-rescued *Raldh2*⁻/⁻ embryos. (A-D) Whole-mount in situ analysis of *EphA4* (A,B) and *EphA2* (C,D) transcripts in E9.5 wild-type (A,C) and *Raldh2*⁻/⁻ (B,D) embryos. In (D), *EphA2*-labeled cells are confined dorsally to the foregut pocket (arrowhead). E-I, Distribution of *Crabp1* transcripts in E9.5 wild-type (E,H) and *Raldh2*⁻/⁻ (F,G,I) embryos. (E-G) Profile and (H,I) dorsal views. Brackets in F,G delineate the mutant post-otic NCC populations (which normally would colonize the 3rd, 4th and 6th branchial arches). An asterisk in G indicates cells that are abnormally confined along the dorsal foregut wall, and may correspond in part to pre-otic (r4-derived) NCC. Mutant embryos also exhibit abnormal patterns of connectivity between the post-otic hindbrain and NCCs (arrowheads and bracket in H and I, respectively). b1-b6, branchial arches; fg, foregut; fl, forelimb bud; ot, otocyst; p1-p3, pharyngeal pouches; r3-r6, rhombomeres.
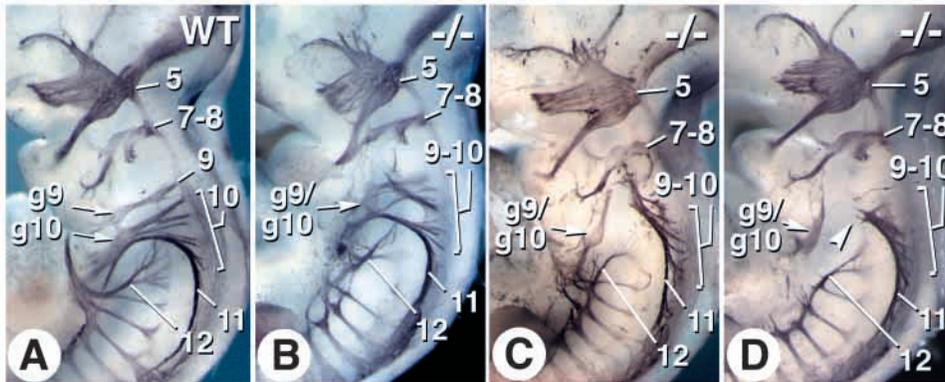
Fig. 5. Growth and patterning defects of posterior cranial nerves in RA-rescued *Raldh2*^{-/-} mutants. Whole-mount anti-neurofilament stainings of E11.5 embryos were examined after removal of the surface ectoderm to expose the nerve tracts. (A) wild-type embryo. (B-D) *Raldh2*^{-/-} embryos with increasingly severe phenotypic defects. Cranial nerves are indicated in Arabic numerals (5-12). g9-g10, distal sensory ganglia of the 9th and 10th nerves, respectively. The arrowhead in D points to an aborted 9th-11th common axonal tract.

5C) or failed to extend towards the periphery (Fig. 5D, arrowhead). In such severe cases, a putative distal ganglion was formed (d9/10 in Fig. 5C,D), which had no connection with the proximal axonal trunk. This indicates that neuronal differentiation could proceed within the mutant epibranchial placodes, but that these neurons were unable to establish a connection with the hindbrain-derived nerve tracts. Altered outgrowth of the 11th (spinal accessory) and 12th (hypoglosseal) nerve tracts was also evident in mutants (Fig. 5B-D). The same range of abnormal phenotypes was observed in *Raldh2*^{-/-} embryos when RA supplementation was extended up to E11.5 (data not shown).

Hindbrain patterning is rescued in RA-supplemented *Raldh2*^{-/-} embryos

In the absence of RA supplementation, *Raldh2*^{-/-} embryos exhibit severe growth and patterning defects of the posterior (prospective r3-r8) hindbrain region (Niederreither et al., 2000). These defects were partly reverted by maternal RA supplementation through oral gavage (Niederreither et al., 2000). Several rhombomeric markers were used to investigate hindbrain patterning in *Raldh2*^{-/-} mutants after RA supplementation from E7.5 to E9.5. *Hoxb1* expression in r4 was comparable in both wild-type and *Raldh2*^{-/-} embryos (Fig. 3A,B). As in wild-type embryos, *Hoxa2* was expressed at higher levels in r3 and (to a lesser extent) r5, and at low levels in r2 and r4 (Fig. 6A,B). Furthermore, *kreisler* expression in r5 and r6 was comparable in wild-type and *Raldh2*^{-/-} embryos [Fig. 6C,D; note, however, that the *kreisler*-labeled NCCs, which normally migrate towards the 3rd branchial arch (Fig. 6C), are deficient in the mutant]. We therefore conclude that hindbrain patterning is efficiently rescued in *Raldh2*^{-/-} embryos through maternal dietary RA supplementation, and that the NCC and cranial nerve abnormalities described above are unlikely to result from defect(s) intrinsic to the hindbrain neuroepithelium.

Rescued *Raldh2*^{-/-} mutants lack enteric nervous system development

The proto-oncogene *Ret* exhibits sequential expression within the NCC components of the developing cranial nerve ganglia. At E9.5, expression is detected in wild-type embryos within the facial-acoustic (7th-8th), glossopharyngeal (9th) and vagal (10th) nerve ganglia (Pachnis et al., 1993) (Fig. 6E). While *Ret* was normally expressed in the facial-acoustic ganglion complex of the RA-rescued *Raldh2*^{-/-} mutants, very few

positive cells were detected posteriorly to the otocyst, at the expected level of the glossopharyngeal and vagal ganglia (Fig. 6F, bracket).

At later stages, *Ret* is specifically expressed in various NCC populations of neural fate, including the vagal NCCs that will give rise to the ganglia of the enteric nervous system
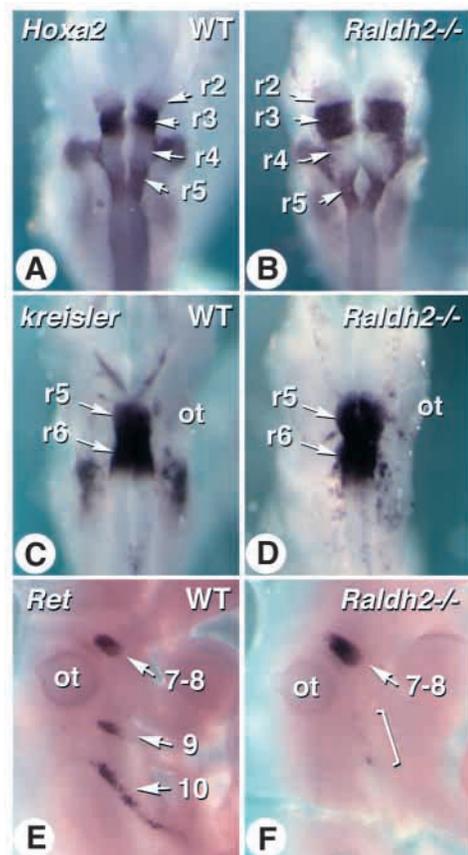

Fig. 6. Rhombomere and cranial ganglion patterning in RA-rescued *Raldh2*^{-/-} embryos. (A-D) *Hoxa2* and *kreisler* rhombomeric transcript patterns were analyzed in E8.5 wild-type (A,C) and *Raldh2*^{-/-} (B,D) embryos (dorsal views). (E,F) Analysis of *Ret* transcripts, which mark the prospective cranial ganglia NCCs in E9.5 wild-type embryos (E), reveals a selective deficiency of the 9th and 10th ganglion cells in mutant embryos (F, a bracket indicates the few post-otic *Ret*-labeled cells). ot, otocyst; r2-r6, rhombomeres; 7-8, 9, 10, prospective cranial nerve ganglia.

(Pachnis et al., 1993). This cell population was analyzed in *Raldh2*$^{-/-}$ mutants by in situ hybridization of serial histological sections. At E10.5, *Ret*-positive prospective enteric ganglioblasts are migrating along the wall of the fore- and midgut of wild-type embryos (Fig. 7A). Only few *Ret*-positive presumptive ganglioblasts were seen in *Raldh2*$^{-/-}$ embryos after RA rescue from E7.5 to E9.5, and these cells were confined to the pharyngeal region and/or the nearby foregut wall (Fig. 7B). By E12.5, the vagal nerves are strongly labeled (Fig. 7C) and the enteric ganglioblasts are beginning to coalesce along the stomach and gut wall to form ganglia in wild-type embryos (Fig. 7E,G). In contrast, the stomach and gut wall of *Raldh2*$^{-/-}$ embryos was devoid of *Ret*-expressing cells (Fig. 7F,H). A few *c-ret*-expressing cells, arranged as rudimentary tracts, were detected at the expected location of the vagal nerves in mutants (compare Fig. 7C and D). Other domains of *Ret* expression were unaltered in *Raldh2*$^{-/-}$ embryos, both in the case of non-NCC (e.g. the ureteric bud or spinal cord motoneurons: Fig. 7A,B and C-F, respectively) and NCC-derived populations (e.g. the dorsal root or trigeminal ganglia: Fig. 7C-F and I,J, respectively). This abnormal phenotype was confirmed by analyzing another marker of the developing enteric nervous system (*Mash1*) (Blaugrund et al., 1996) (data not shown). Extending the RA supplementation until E12.5 did not rescue the formation of enteric ganglia in *Raldh2*$^{-/-}$ mutants. In the best case, labeled cells were found along part of the foregut and stomach wall, but these cells did not colonize more posterior gut segments (data not shown).

DISCUSSION

RA-dependent development of posterior pharyngeal arches cannot be rescued in *Raldh2*-null mutants by maternal RA supplementation

Our analyses have revealed altered migration patterns of the post-otic hindbrain neural crest cells (NCC), which normally give rise to the cardiac NCC population, in the RA-rescued *Raldh2*$^{-/-}$ embryos. We show that these NCC defects are part of a complex range of alterations that encompass the whole posterior pharyngeal region. Whereas the first and second branchial arches form properly, development of the 3rd to 6th branchial arches and their derivatives (aortic arches, cranial nerves) is severely impaired in mutant embryos. Most notably, pharyngeal pouches fail to form within the posterior pharyngeal endoderm and development of the corresponding pouch-derived organs, such as the thymus and parathyroid glands, is compromised. Furthermore, a single (sometimes rudimentary) arterial vessel is formed instead of the 3rd to 6th aortic arches. This arterial defect likely accounts for the death of some of the rescued mutants prior to fetal stages. Indeed, PTA as an isolated malformation is not lethal until after birth (Larsen, 1993), whereas the observed aortic arch defect may compromise blood circulation in the mutant embryos as soon as their 1st and 2nd arches regress and are remodelled.

Using several hindbrain markers, we show that growth and patterning of the posterior rhombomeres, which is highly abnormal in unrescued *Raldh2*$^{-/-}$ embryos (Niederreither et al., 2000), is rescued by the present maternal RA supplementation.
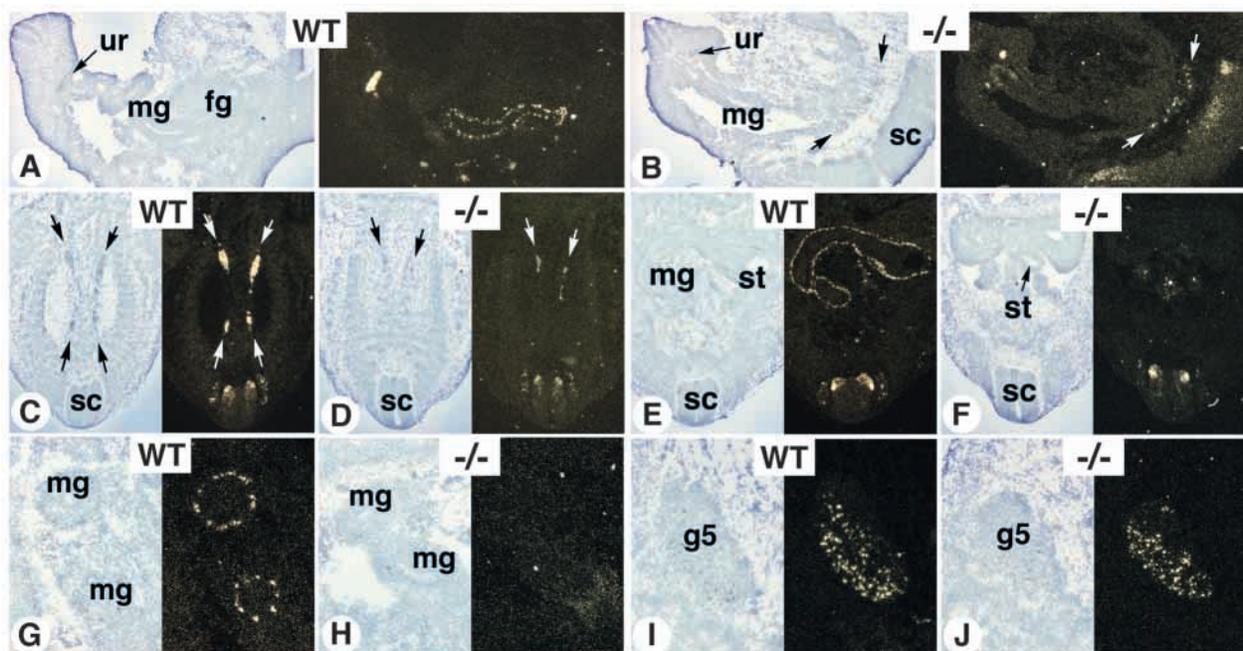

Fig. 7. Lack of enteric nervous system development in RA-rescued *Raldh2*$^{-/-}$ mutants. In situ hybridization was performed with a ^{35}S-labeled *Ret* probe on cryosections of wild-type (A,C,E,G,I) and *Raldh2*$^{-/-}$ (B,D,F,H,J) embryos. Each panel shows bright-field (left) and dark-field (right) views of the same section to show, respectively, the histology and the in situ hybridization signal (white dots). At E10.5, mutant embryos only show scattered *Ret*-labeled prospective ganglioblasts (arrows in B), which failed to colonize the midgut levels (compare A and B). E12.5 mutant embryos have rudimentary vagal nerve tracts (compare C and D, arrows) and their stomach and gut wall are devoid of *Ret*-positive ganglion cells (compare E,G and F,H). Other domains of *Ret* expression (e.g. in the trigeminal ganglia: compare I and J) are unaffected in mutants. fg, foregut; g5, trigeminal ganglion; mg, midgut; sc, spinal cord; st, stomach; ur, ureteric bud.

It is therefore likely that the abnormal NCC migration patterns observed in RA-rescued *Raldh2*-null mutants are secondary to the abnormal development of the pharyngeal region, rather than being the result of an intrinsic hindbrain or NCC defect.

Our data show that RALDH2 is responsible for producing RA which is required for proper development of the posterior branchial arch region. Previous studies have indicated that this embryonic region is particularly sensitive to RA deficiency. Incubation of early somite-stage (E8.0-8.5) cultured mouse embryos with a pan-RAR antagonist led to defects of the 3rd to 6th branchial arch region (Wendling et al., 2000), which are consistent with those seen in RA-rescued *Raldh2*-null mutants. Furthermore, vitamin A-deficient (VAD) quail embryos exhibit deficits in the posterior pharyngeal region (Quinlan et al., 2002), which are reminiscent of the mouse phenotype in these experiments. For instance, both the VAD quail embryos and the rescued *Raldh2* mouse mutants develop a rather normal first pharyngeal pouch, whereas only a single, abnormal second pouch is formed posteriorly. In agreement with these studies (Wendling et al., 2000; Quinlan et al., 2002), our data point to the pharyngeal endoderm as one of the main target tissues whose patterning is altered by conditions of impaired RA signaling.

We have shown that *Raldh2* expression is mesoderm-specific, and is restricted to the posteriormost pharyngeal region during development of the posterior branchial arches. We propose that RALDH2 function is to produce locally high amounts of RA, which are indispensable to correctly pattern these branchial arches. The mesodermally produced RA would then diffuse and signal within the pharyngeal endoderm. This is illustrated by the fact that activity of a RARE-*lacZ* reporter transgene, as well as endogenous expression of RA target genes (such as *Hoxa1* and *Hoxb1*), is induced in both the mesoderm and endoderm of the posterior pharyngeal region. In the rescued *Raldh2*-null mutants, RA brought transplacentally cannot mimic the levels and distribution resulting from endogenous, RALDH2-mediated synthesis, leading to region-specific defects. Interestingly, these mutants exhibit a decrease of RA-reporter transgene activity in both the pharyngeal mesoderm and endoderm. Expression levels of *Hoxa1* and *Hoxb1* are decreased in mesoderm and endoderm as well, demonstrating that both layers are deficient in their response to the RA signal.

We have also found that development of the 2nd branchial arches, which is deficient in the *Raldh2*-null mutants (Niederreither et al., 1999), is efficiently rescued by maternal RA supplementation. This indicates that 2nd arch development may require lower RA levels, which can be supplied maternally in the absence of RALDH2 function. Other lines of evidence, involving analysis of RAR compound mutant mice (Lohnes et al., 1994), VAD rat embryos (White et al., 2000) or pan-RAR antagonist-treated mouse embryos (Wendling et al., 2000), have indicated that development of the 2nd branchial arches is not as critically dependent on RA signaling as that of more posterior arches. Whether this differential requirement reflects binding to a different subset of receptors has been discussed elsewhere (Wendling et al., 2000). We postulate that RA produced by RALDH2 in the posterior pharyngeal mesoderm diffuses up to the level of the 2nd branchial arches, where its acts at relatively lower concentrations. This is supported by the pattern of activity of the RARE-*lacZ* reporter transgene which,

in wild-type embryos, extends up to the developing 2nd arches, albeit at a much lower level than in the posterior pharyngeal region.

The rescued *Raldh2*-null phenotype resembles human DiGeorge syndrome and mouse *Tbx1* knockout phenotypes

Conotruncal abnormalities are prevalent human birth defects occurring at a frequency as high as four per 10,000 births. As many congenital defects, the origins of PTA are often unknown. Poor nutrition during pregnancy – including vitamin A deficiency – may contribute to these malformations (Underwood and Arthur, 1996). The most frequent genetic cause of human conotruncal defects consists of heterozygous microdeletions of the chromosome 22q11 region, which lead to a spectrum of abnormalities of variable expressivity, known as DiGeorge/Velocardiofacial syndromes (DGS/VCFS) (reviewed by Scambler, 2000; Emanuel, 2001; Lindsay, 2001). Several engineered deletions of the corresponding mouse locus have implicated the T-box gene *Tbx1* as a major determinant of the DGS/VCFS phenotypes (Jerome and Papaioannou, 2001; Lindsay et al., 2001; Merscher et al., 2001). Both haploinsufficient and null (*Tbx1$^{-/-}$*) mutant mice fail to form the 3rd and 4th pharyngeal arches and have conotruncal defects (Lindsay et al., 2001; Jerome and Papaioannou, 2001; Merscher et al., 2001). Alterations in thymus and parathyroid morphology are also seen in these mutants (Jerome and Papaioannou, 2001; Merscher et al., 2001). According to its expression which is essentially restricted to the pharyngeal pouch endoderm, *Tbx1* appears to function in a non-cell autonomous manner for branchial arch outgrowth, and NCC defects in these mutants have been attributed to a lack of guidance from the pouch endoderm (Vitelli et al., 2002).

The defects reported in the present study are clearly similar to those observed in posterior branchial arches (and their derivatives) in *Tbx1* mutant mice, and therefore represent a new mouse model of the human DGS abnormalities. The pharyngeal region appears to be highly sensitive to alterations in RA levels, as a hypomorphic mouse *Raldh2* mutation was found to selectively lead to DGS-like defects (Vermot et al., 2003), albeit less severe than in the present *Raldh2*-null mutants. As *Tbx1* expression is not (or only mildly) affected in both the null (data not shown) and hypomorphic (Vermot et al., 2003) mutants, we do not consider it as a critical determinant of the *Raldh2* phenotype. It rather seems that RA may act downstream (or in combination with) TBX1 to regulate expression of signaling molecules required for proper pharyngeal development. FGF8 could represent such a critical common downstream signal, as (i) its expression is altered in both *Tbx1$^{-/-}$* and *Raldh2$^{-/-}$* mutants (Vitelli et al., 2002) (this study), and (ii) its hypomorphic mutation also leads to a DGS-like phenotype (Abu-Issa et al., 2002; Frank et al., 2002).

Lack of vagal outgrowth leads to absence of the enteric nervous system

Retinoic acid has been implicated in the regulation of many aspects of neuronal development including specification of neuronal cell fate (Sockanathan and Jessell, 1998) and stimulation of neurite outgrowth (Hunter et al., 1991; Plum and Clagett-Dame, 1996; Corcoran and Maden, 1999). RA has also been found to promote survival and proliferation of neuronal

progenitors in NCC populations (Henion and Weston, 1994; Gale et al., 1996). We find that axonal growth is variably affected at the level of the posterior (9th-12th) cranial nerves in RA-rescued *Raldh2*$^{-/-}$ mutants (see Fig. 4), consistent with the idea that RA produced locally by RALDH2 in the pharyngeal mesoderm is required to stimulate their neurite outgrowth.

The enteric nervous system (ENS) is mainly derived from vagal NCCs, which migrate along the foregut mesenchyme to colonize the entire length of the gut and give rise to the majority of neurons and glia of the enteric ganglia (Le Douarin and Teillet, 1973; Young et al., 1998; Burns and Le Douarin, 1998). Among the signaling pathways involved in ENS development (for reviews, see Gershon, 1998; Taraviras and Pachnis, 1999), the RET receptor tyrosine kinase and its ligand GDNF (glial cell line-derived neurotrophic factor) are of critical importance. Both *Ret* and *Gdnf* knockout mice exhibit semi-dominant hypo- or aganglionosis of the gastrointestinal tract (Schuchardt et al., 1995; Pichel et al., 1996; Shen et al., 2002). RET mutations are also most frequently involved in cases of human Hirschprung's disease (congenital megacolon or aganglionosis), the most frequent hereditary cause of intestinal obstruction (Gabriel et al., 2002). Here we show that the vagal defects in *Raldh2*$^{-/-}$ embryos lead to a similar gastrointestinal aganglionic phenotype. While few *Ret*-positive ENS progenitor cells are detected along the foregut wall at E10.5, they are apparently unable to colonize the gastrointestinal tract, leading to an absence of enteric ganglia. This is the first report of intestinal agangliogenesis caused by an alteration in the retinoid signaling pathway. The possibility that such alterations could be involved in the pathogeny of human Hirschprung's disease, which is both variable in its expressivity and complex in its inheritance pattern, should therefore be considered.

REFERENCES

Abu-Issa, R., Smyth, G., Smoak, I., Yamamura, K. and Meyers, E. N. (2002). Fgf8 is required for pharyngeal arch and cardiovascular development in the mouse. *Development* **129**, 4613-4625.

Blaugrund, E., Pham, T. D., Tennyson, V. M., Lo, L., Sommer, L., Anderson, D. J. and Gershon, M. D. (1996) Distinct subpopulations of enteric neuronal progenitors defined by time of development, sympathoadrenal lineage markers and Mash-1-dependence. *Development* **122**, 309-320.

Burns, A. J. and Douarin, N. M. (1998). The sacral neural crest contributes neurons and glia to the post-umbilical gut: spatiotemporal analysis of the development of the enteric nervous system. *Development* **125**, 4335-4347.

Chambon, P. (1996). A decade of molecular biology of retinoic acid receptors. *FASEB J.* **10**, 940-954.

Corcoran, J. and Maden, M. (1999). Nerve growth factor acts via retinoic acid synthesis to stimulate neurite outgrowth. *Nat. Neurosci.* **2**, 307-308.

Creazzo, T. L., Godt, R. E., Leatherbury, L., Conway, S. J. and Kirby, M. L. (1998). Role of cardiac neural crest cells in cardiovascular development. *Annu. Rev. Physiol.* **60**, 267-286.

Crossley, P. H. and Martin, G. R. (1995). The mouse Fgf8 gene encodes a family of polypeptides and is expressed in regions that direct outgrowth and patterning in the developing embryo. *Development* **121**, 439-451.

Décimo, D., Georges-Labouesse, E. and Dollé, P. (1995). In situ hybridization to cellular RNA. In *Gene Probes 2, a Practical Approach*, pp. 183-210. New York: Oxford University Press.

Dupé, V., Ghyselinck, N. B., Wendling, O., Chambon, P. and Mark, M. (1999). Key roles of retinoic acid receptors alpha and beta in the patterning of the caudal hindbrain, pharyngeal arches and otocyst in the mouse. *Development* **126**, 5051-5059.

Emanuel, B. S., McDonald-McGinn, D., Saitta, S. C. and Zackai, E. H. (2001). The 22q11.2 deletion syndrome. *Adv. Pediatr.* **48**, 39-73.

Frank, D. U., Fotheringham, L. K., Brewer, J. A., Muglia, L. J., Tristani-Firouzi, M., Capecchi, M. R. and Moon, A. M. (2002). An Fgf8 mouse mutant phenocopies human 22q11 deletion syndrome. *Development* **129**, 4591-4603.

Gabriel, S. B., Salomon, R., Pelet, A., Angrist, M., Amiel, J., Fornage, M., Attie-Bitach, T., Olson, J. M., Hofstra, R., Buys, C. et al. (2002). Segregation at three loci explains familial and population risk in Hirschsprung disease. *Nat. Genet.* **31**, 89-93.

Gale, E., Prince, V., Lumsden, A., Clarke, J., Holder, N. and Maden, M. (1996). Late effects of retinoic acid on neural crest and aspects of rhombomere. *Development* **122**, 783-793.

Gavalas, A., Studer, M., Lumsden, A., Rijli, F. M., Krumlauf, R. and Chambon, P. (1998). Hoxa1 and Hoxb1 synergize in patterning the hindbrain, cranial nerves and second pharyngeal arch. *Development* **125**, 1123-1136.

Gershon, M. D. (1998). V. Genes, lineages and tissue interactions in the development of the enteric nervous system. *Am. J. Physiol.* **275**, 869-873.

Ghyselinck, N. B., Wendling, O., Messaddeq, N., Dierich, A., Lampron, C., Décimo, D., Viville, S., Chambon, P. and Mark, M. (1998). Contribution of retinoic acid receptor beta isoforms to the formation of the conotruncal septum of the embryonic heart. *Dev. Biol.* **198**, 303-318.

Henion, P. D. and Weston, J. A. (1994). Retinoic acid selectively promotes the survival and proliferation of neurogenic precursors in cultured neural crest cell populations. *Dev. Biol.* **161**, 243-250.

Hunter, K., Maden, M., Summerbell, D., Eriksson, U. and Holder, N. (1991). Retinoic acid stimulates neurite outgrowth in the amphibian spinal cord. *Proc. Natl. Acad. Sci. USA* **88**, 3666-3670.

Jerome, L. A. and Papaioannou, V. E. (2001). DiGeorge syndrome phenotype in mice mutant for the T-box gene, Tbx1. *Nat. Genet.* **27**, 286-291.

Jiang, X., Rowitch, D. H., Soriano, P., McMahon, A. P. and Sucov, H. M. (2000). Fate of the mammalian cardiac neural crest. *Development* **127**, 1607-1616.

Kirby, M. L. (1998). Contribution of neural crest to heart and vessel morphology. In *Heart Development* (ed. R. P. Harvey and N. Rosenthal), p. 179. San Diego: Academic Press.

Larsen, W. J. (1997). *Human Embryology*. New York, NY: Churchill Livingstone.

Le Douarin, N. M. and Teillet, M. A. (1973). The migration of neural crest cells to the wall of the digestive tract in avian embryo. *J. Embryol. Exp. Morphol.* **30**, 31-48.

Lindsay, E. A. (2001). Chromosomal microdeletions: dissecting del22q11 syndrome. *Nat. Rev. Genet.* **2**, 858-868.

Lindsay, E. A., Vitelli, F., Su, H., Morishima, M., Huynh, T., Pramparo, T., Jurecic, V., Ogunrinu, G., Sutherland, H. F., Scambler, P. J. et al. (2001). Tbx1 haploinsufficiency in the DiGeorge syndrome region causes aortic arch defects in mice. *Nature* **410**, 97-101.

Lohnes, D., Mark, M., Mendelsohn, C., Dolle, P., Dierich, A., Gorry, P., Gansmuller, A. and Chambon, P. (1994). Function of the retinoic acid receptors (RARs) during development (I). Craniofacial and skeletal abnormalities in RAR double mutants. *Development* **120**, 2723-2748.

Maden, M., Horton, C., Graham, A., Leonard, L., Pizzey, J., Siegenthaler, G., Lumsden, A. and Eriksson, U. (1992). Domains of cellular retinoic acid-binding protein I (CRABP I) expression in the hindbrain and neural crest of the mouse embryo. *Mech. Dev.* **37**, 13-23.

Mangelsdorf, D. J. (1994). Vitamin A receptors. *Nutr. Rev.* **52**, S32-44.

Mark, M., Lufkin, T., Vonesch, J. L., Ruberte, E., Olivo, J. C., Dollé, P., Gorry, P., Lumsden, A. and Chambon, P. (1993). Two rhombomeres are altered in Hoxa-1 mutant mice. *Development* **119**, 319-338.

Mendelsohn, C., Lohnes, D., Décimo, D., Lufkin, T., LeMeur, M.,

Chambon, P. and Mark, M. (1994). Function of the retinoic acid receptors (RARs) during development. II. Multiple abnormalities at various stages of organogenesis in RAR double mutants. *Development* **120**, 2749-2771.

Merscher, S., Funke, B., Epstein, J. A., Heyer, J., Puech, A., Lu, M. M., Xavier, R. J., Demay, M. B., Russell, R. G., Factor, S. et al. (2001). TBX1 is responsible for cardiovascular defects in velo-cardio-facial/DiGeorge syndrome. *Cell* **104**, 619-629.

Müller, T. S., Ebensperger, C., Neubuser, A., Koseki, H., Balling, R., Christ, B. and Wilting, J. (1996). Expression of avian Pax1 and Pax9 is intrinsically regulated in the pharyngeal endoderm, but depends on environmental influences in the paraxial mesoderm. *Dev. Biol.* **178**, 403-417.

Niederreither, K. and Dollé, P. (1998). In situ hybridization with ^{35}S-labelled probes for retinoid receptors. In *Methods in Molecular Biology: Retinoids* (ed. C. P. F. Redfern), pp. 247-267. Totowa: Humana Press.

Niederreither, K., McCaffery, P., Dräger, U. C., Chambon, P. and Dollé, P. (1997). Restricted expression and retinoic acid-induced downregulation of the retinaldehyde dehydrogenase type 2 (RALDH-2) gene during mouse development. *Mech. Dev.* **62**, 67-78.

Niederreither, K., Subbarayan, V., Dollé, P. and Chambon, P. (1999). Embryonic retinoic acid synthesis is essential for early mouse post-implantation development. *Nature Genet*. **21**, 444-448.

Niederreither, K., Vermot, J., Schuhbaur, B., Chambon, P. and Dollé, P. (2000). Retinoic acid synthesis and hindbrain patterning in the mouse embryo. *Development* **127**, 75-85.

Niederreither, K., Vermot, J., Messaddeq, N., Schuhbaur, B., Chambon, P. and Dollé, P. (2001). Embryonic retinoic acid synthesis is essential for heart morphogenesis in the mouse. *Development* **128**, 1019-1031.

Niederreither, K., Vermot, J., Fraulob, V., Chambon, P. and Dollé, P. (2002). Retinaldehyde dehydrogenase 2 (RALDH2) independent patterns of retinoic acid synthesis in the mouse embryo. *Proc. Natl. Acad. Sci. USA* **99**, 16111-16116.

Nieto, M. A., Gilardi-Hebenstreit, P., Charnay, P. and Wilkinson, D. G. (1992). A receptor protein tyrosine kinase implicated in the segmental patterning of the hindbrain and mesoderm. *Development* **116**, 1137-1150.

Pachnis, V., Mankoo, B. and Costantini, F. (1993). Expression of the c-ret proto-oncogene during mouse embryogenesis. *Development* **119**, 1005-1017.

Pichel, J. G., Shen, L., Sheng, H. Z., Granholm, A. C., Drago, J., Grinberg, A., Lee, E. J., Huang, S. P., Saarma, M., Hoffer, B. J., Sariola, H. and Westphal, H. (1996). Defects in enteric innervation and kidney development in mice lacking GDNF. *Nature* **382**, 73-76.

Plum, L. A. and Clagett-Dame, M. (1996). All-trans retinoic acid stimulates and maintains neurite outgrowth in nerve growth factor-supported developing chick embryonic sympathetic neurons. *Dev. Dyn.* **205**, 52-63.

Quinlan, R., Gale, E., Maden, M. and Graham, A. (2002). Deficits in the posterior pharyngeal endoderm in the absence of retinoids. *Dev. Dyn.* **225**, 54-60.

Rossant, J., Zirngibl, R., Cado, D., Shago, M. and Giguere, V. (1991). Expression of a retinoic acid response element-hsplacZ transgene defines specific domains of transcriptional activity during mouse embryogenesis. *Genes Dev.* **5**, 1333-1344.

Ruiz, J. C. and Robertson, E. J. (1994). The expression of the receptor-protein tyrosine kinase gene, eck, is highly restricted during early mouse development. *Mech. Dev.* **46**, 87-100.

Scambler, P. J. (2000). The 22q11 deletion syndromes. *Hum. Mol. Genet.* **9**, 2421-2426.

Schuchardt, A., Srinivas, S., Pachnis, V. and Costantini, F. (1995). Isolation and characterization of a chicken homolog of the c-ret proto-oncogene. *Oncogene* **10**, 641-649.

Shen, L., Pichel, J. G., Mayeli, T., Sariola, H., Lu, B. and Westphal, H. (2002). Gdnf haploinsufficiency causes Hirschsprung-like intestinal obstruction and early-onset lethality in mice. *Am. J. Hum. Genet.* **70**, 435-447.

Sockanathan, S. and Jessel, T. M. (1998). Motor neuron-derived retinoid signaling specifies the subtype identity of spinal motor neurons. *Cell* **94**, 503-514.

Taraviras, S. and Pachnis, V. (1999). Development of the mammalian enteric nervous system. *Curr. Opin. Genet. Dev.* **9**, 321-327.

Underwood, B. A. and Arthur, P. (1996). The contribution of vitamin A to public health. *FASEB J.* **10**, 1040-1048.

Vermot, J., Niederreither, K., Garnier, J. M., Chambon, P. and Dollé, P. (2003). Decreased embryonic retinoic acid synthesis results in a DiGeorge syndrome phenotype in newborn mice. *Proc. Natl. Acad. Sci. USA* **100**, 1763-1768.

Vitelli, F., Taddei, I., Morishima, M., Meyers, E. N., Lindsay, E. A. and Baldini, A. (2002). A genetic link between Tbx1 and fibroblast growth factor signaling. *Development* **129**, 4605-4611.

Wall, N. A. and Hogan, B. L. (1995). Expression of bone morphogenetic protein-4 (BMP-4), bone morphogenetic protein-7 (BMP-7), fibroblast growth factor-8 (FGF-8) and sonic hedgehog (SHH) during branchial arch development in the chick. *Mech. Dev.* **53**, 383-392.

Wendling, O., Dennefeld, C., Chambon, P. and Mark, M. (2000). Retinoid signaling is essential for patterning the endoderm of the third and fourth pharyngeal arches. *Development* **127**, 1553-1562.

White, J. C., Highland, M., Kaiser, M. and Clagett-Dame, M. (2000). Vitamin A deficiency results in the dose-dependent acquisition of anterior character and shortening of the caudal hindbrain of the rat embryo. *Dev. Biol.* **220**, 263-284.

Wilson, J. G. and Warkany, J. (1949). Aortic arch and cardiac anomalies in the offspring of vitamin A deficient rats. *Am. J. Anat.* **85**, 113-155.

Young, H. M., Torihashi, S., Ciampoli, D. and Sanders, K. M. (1998). Identification of neurons that express stem cell factor in the mouse small intestine. *Gastroenterology* **115**, 898-908.